Available online at www.sciencedirect.com
SCIENCE DIRECT®
Journal of Nuclear Materials 337–339 (2005) 722–726
journal of nuclear materials
www.elsevier.com/locate/jnucmat

Determination of the particle and energy fluxes in the JET far SOL during ELMs using the reciprocating probe diagnostic

C. Silva [a,*], B. Gonçalves [a], C. Hidalgo [b], K. Erents [c], A. Loarte [d], G. Matthews [c], M. Pedrosa [b]

[a] *Associação Euratom/IST, Centro de Fusão Nuclear, Instituto Superior Técnico, 1049-001 Lisboa, Portugal*
[b] *Associación Euratom/Ciemat, 28040 Madrid, Spain*
[c] *Euratom/UKAEA Association, Culham Science Centre, Abingdon, Oxon OX14 3DB, UK*
[d] *EFDA-Garching, Max-Planck-Institut für Plasmaphysik, Germany*

Abstract

The effect of ELMs on the JET far SOL plasma parameters has been investigated using a multi-pin system. It has been observed that the effective radial transport of particles increases with the ELM size. In spite of the large particle flux measured in the far SOL plasma during type I ELMs, the energy carried by electrons to the main chamber PFCs is very small (<5% of the ELM losses).

PACS: 52.40.Hf; 52.25.Fi; 52.35.Ra
Keywords: ELM, Particle and heat transport; Plasma turbulence; Reciprocating probe; Power exhaust

1. Introduction

Edge localized modes (ELMs) lead to high transient heat and particle loads on the plasma facing components (PFCs). In between ELMs most of the energy transported across the separatrix onto the scrape-off layer (SOL) is deposited in the divertor targets. However, there are indications that during ELMs a significant part of the energy may be deposited outside the divertor region [1,2 and references therein]. This enhancement of the plasma-wall interactions during ELMs may influence the lifetime of main chamber PFCs in ITER and the core plasma impurity contamination. The JET Reciprocating probe data show that the far SOL particle flux strongly increases during ELMs, implying that the ELM convective SOL-width is much broader than that measured in between ELMs. The main objective of this work is to measure the particle flux as well as the heat flux in the far SOL and to investigate the variation of the radial transport with the ELMs characteristics.

Data obtained with a multi-probe system has been used previously on JET to study the radial propagation of ELMs in the SOL region [3]. It has been shown that the ELM event propagates with an effective radial velocity in the range of 1000 m/s, suggesting that the ELM arrival time to the main chamber PFCs can be comparable to the characteristic time of transport to the divertor. Analysis of the JET outboard limiter Langmuir probes data also revealed significant ELM interaction with the outboard limiter and similar radial propagation

* Corresponding author. Tel.: +351 21 8419113; fax: +351 21 8417819.
E-mail address: csilva@cfn.ist.utl.pt (C. Silva).

0022-3115/$ - see front matter © 2004 Elsevier B.V. All rights reserved.
doi:10.1016/j.jnucmat.2004.09.052

velocities were found [4]. Reciprocating probes have also been used on DIII-D [5–7] and MAST [8] to investigate transport in the close and far SOL during ELMs. A significant structure of the ELM perturbation was found and large radial velocities inferred. The ELM heat pulse was found to be not a single pulse but a series of strong, short bursts [7]. Furthermore, the particle and heat flux have been measured in the boundary plasma of the DIII-D tokamak with high temporal and spatial resolution and results indicated that particles are transported radially much more efficiently than heat [6,7].

2. Experimental set-up

The principal diagnostic used in this work has been a 9-pin probe head mounted onto a fast reciprocating drive system that inserts the probe into the plasma vertically near the top of the plasma. A poloidal cross-section of the plasma showing the probe position together with the relevant lines of sight of the D_α detectors is presented in Fig. 1. The probe system presently installed at JET allows the simultaneous measurement of the ion saturation current, I_{sat}, floating potential, V_f, electron temperature, T_e, and turbulent driven particle and energy flux with a high temporal resolution (500 kHz). The electron temperature has been evaluated using a modified triple probe method where one tip was operated at a fixed applied voltage (V_{ap}) and the remaining two tips measured V_f and I_{sat} [9]. The electron temperature may be therefore obtained using $T_e = (V_{ap} - V_f)/\ln\left(1 - I_{V_{ap}}/I_{sat}\right)$.

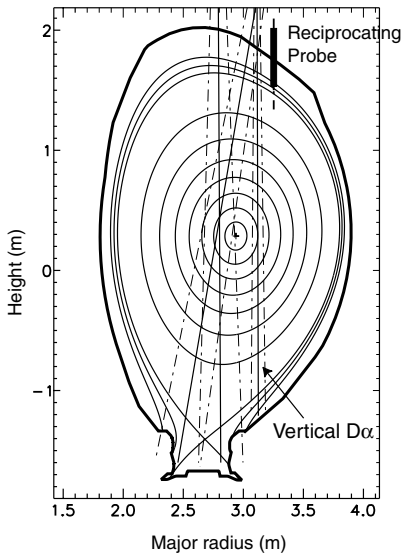

Fig. 1. A poloidal cross-section of the plasma showing the probe position together with the relevant lines of sight of the D_α detectors.

3. Experimental results

Fig. 2 shows the time evolution of the reciprocating probe position with respect to the separatrix, the ion saturation current density (J_{sat}) and the outer divertor D_α radiation as the probe is inserted into the plasma for an ELMy H-mode discharge. Small amplitude type I ELMs are clearly seen in the probe signals. In the region outside the limiter radius ($t < 64$ s) the probe signal is very small, while closer to the separatrix we often observed electron emission of the tips ($t \sim 64.035$ s). The particle flux in the far SOL increases significantly during ELMs suggesting that the latter produces an anomalously high cross-field transport and that particles are lost to the main chamber PFCs by perpendicular transport. Furthermore, the J_{sat} signal shows that ELMs have a complex structure, which varies from ELM to ELM.

As illustrated in Fig. 2, type I ELMs are difficult to investigate with the reciprocating probe due to the high energy fluxes associated with them. The probe must be far away from the separatrix, otherwise the tips will emit, but still inside the limiter radius since plasma parameters decay strongly behind that position. The reciprocating probe was only used in a small number of ELMy discharges with different magnetic configurations (not optimised for measurements with the reciprocating probe). Therefore, the present database ($1.5 < I_p < 2.5$ MA, $2.2 < B_T < 3.2$ T, $3.5 < q_{95} < 6.5$, $\Delta W_{ELM} < 150$ kJ, $30 < f_{ELM} < 400$ Hz, ELMs type I and III, $3 < r_{probe} - r_{sep} < 5$ mid-plane cm) does not allow the study of the far SOL parameters dependence

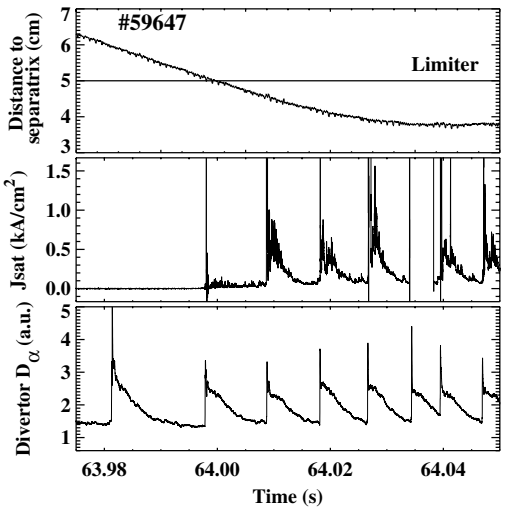

Fig. 2. Time evolution of the reciprocating probe position with respect to the separatrix, J_{sat} and the outer divertor D_α radiation as the probe is inserted into the plasma for a discharge with $I_p = 2$ MA, $B_T = 2.4$ T. The outer limiter position is also indicated.

on the discharge/ELM characteristics apart from the dependence on the ELM frequency. In the following sections the behaviour of the radial velocity, electron temperature and fluctuation driven particle and energy fluxes during ELMs will be presented.

3.1. Particle flux and radial velocity in the far SOL

A clear correlation between the far SOL J_{sat} amplitude ($\propto nT^{1/2}$) and the ELM frequency (f_{ELM}) has been found, as observed before for other edge quantities (e.g. [10]). Fig. 3 shows the dependence of the far SOL J_{sat} due to ELMs ($\langle J_{sat} - J_{sat}^{bef} \rangle^{ELM}$, where J_{sat}^{bef} is the value of J_{sat} just before the ELM and the brackets, $\langle\ \rangle$, denote time average during an ELM) on the ELM frequency. J_{sat} decreases roughly exponentially as the ELM frequency increases in spite of the different main plasma parameters, with a reduction of the slope observed for $f_{ELM} > 300$ Hz. A similar behaviour is observed with the D_α radiation from a detector looking vertically at a poloidal position close to that of the reciprocating probe. When the inner/outer divertor D_α signals are used the scatter is much larger as the divertor radiation depends strongly on the plasma configuration.

An effective radial velocity has been defined as the $E \times B$ turbulent particle transport normalized to the local density, $V_r = \langle \tilde{I}_{sat} \tilde{E}_\theta \rangle / I_{sat} B$, where E_θ is the poloidal electric field estimated from floating potential signals measured by poloidally separated probes and fluctuating quantities are denoted by '~'. Fig. 4 shows the time evolution of I_{sat} and V_r during a type I ELM in the far SOL ($r - r_{sep} \approx 4$ cm). The fast probe data revels that the radial velocity during ELMs has a complex structure

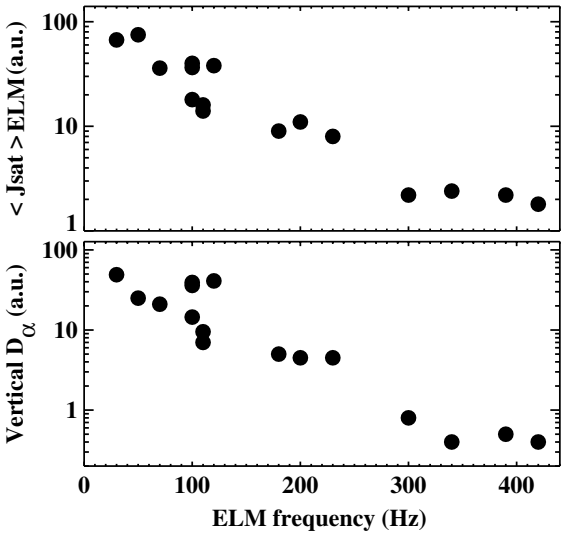

Fig. 3. Dependence of J_{sat} and vertical D_α on the ELM frequency.

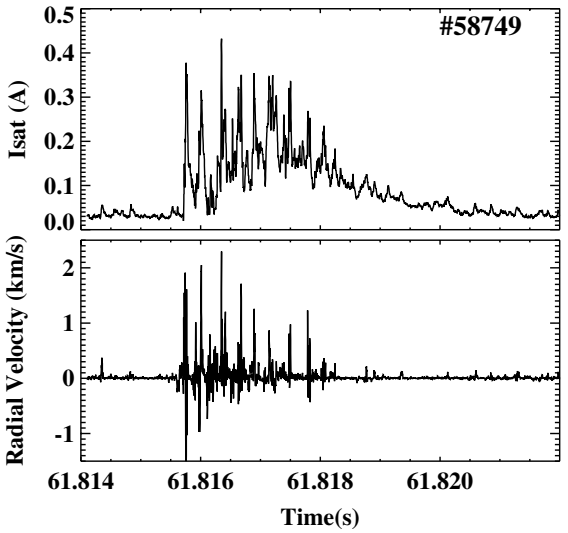

Fig. 4. Time evolution of I_{sat} and the effective radial velocity during an ELM for a discharge with $I_p = 2$ MA, $B_T = 2.45$ T.

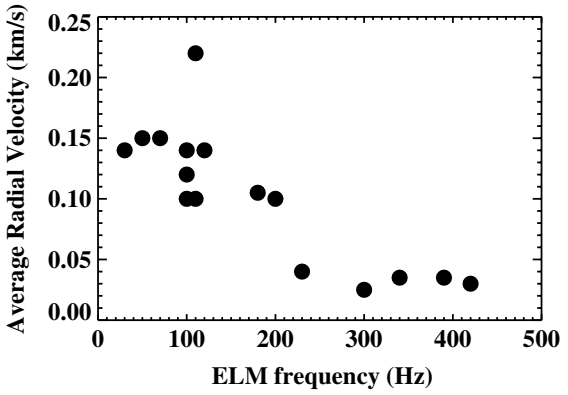

Fig. 5. Dependence of the ELM averaged radial velocity on the ELM frequency.

as observed with the other probe signals. Radial velocities up to 2 km/s are observed in the far SOL, being larger in the beginning of the ELM. These results imply that ELMs arrival time to the limiter surfaces (>50 μs for a typical distance between the separatrix and the outer limiter of 10 cm), can be comparable to, or even smaller than, the characteristic time of transport to the divertor (in the range of 100–500 μs). Fig. 5 illustrates the ELM averaged radial velocity as a function on the ELM frequency showing that the radial velocity decreases as the ELM frequency increases. These results are in agreement with previous findings showing that during ELMs there is a link between radial velocity and the size of transport events (quantified by the local density gradient) [3].

3.2. Determination of the temperature and energy density during ELMs

Fig. 6 illustrates the time evolution of J_{sat}, T_e and fluctuation driven particle and energy fluxes during a small type I ELM at $r - r_{sep} \approx 4$ cm (#58749). For this pulse the ELM frequency is ~50 Hz and the typical energy loss per ELM is ~75 kJ. During the ELM, J_{sat} increases by factor larger than 5 while the electron temperature increases by only a factor of 2. For higher frequency ELMs the electron temperature increase is similar but limited to a few hundred of microseconds. These results show that the high temperature electrons ($T_e > 500$ eV) ejected by the ELM from the pedestal region do not reach the far SOL probably because the electron conduction to the target is very fast [4]. However, there is strong evidence from recent measurement using a retarding field analyser probe in the JET far SOL plasma that during ELMs the energy of ions arriving at the first wall may be significant [11].

The probe arrangement allows the simultaneous measurement of the fluctuations driven particle flux, as well as the convective and conductive components of the electron heat flux, which are respectively given by $\Gamma_r = \frac{1}{B}\langle \tilde{n}\tilde{E}_\theta \rangle$ and $Q_r = Q_{conv} + Q_{cond} = \frac{3}{2}kT_e\Gamma_r + \frac{3}{2}\frac{n_e}{B}\langle k\tilde{T}_e \tilde{E}_\theta \rangle$ [12]. The time evolution of these quantities is also shown in Fig. 6. Before the ELM, both the particle and heat flux in the far SOL are negligible, increasing significantly during the ELM. Probe data reveals again that ELMs have a complex structure, with positive and negative events, the average flux being directed outwards. During ELMs the convective and conductive components of the heat flux have a similar magnitude due to the good correlation between density and temperature fluctuations. In opposition, on DIII-D, particle convection was found to be the main mechanism for radial heat transport during ELMs [6].

In order to evaluate the total energy arriving into the far SOL, toroidal and poloidal symmetry has to be assumed since measurements are made at one location only. However, this is not the case, as the spatial distribution of the ELM losses is believed to be poloidaly localized near the low field side midplane e.g. [5]. Integrating Q_r in time and multiplying by the plasma surface (poloidal symmetry assumed) the total electron energy arriving at the far SOL can be estimated to be ~3 kJ. Due to the assumptions made, the calculated heat flux has large error bars. However, we may conclude that the heat flux is very small when compared with the ELM energy loss (~75 kJ). These results are in agreement with similar measurements done on DIII-D where it was also found that particles are transported radially much more efficiently than heat [6].

4. Discussion and conclusions

Probe data presented in Section 3.1 show that the effective radial transport of particles is larger for the large amplitude ELMs. Results indicate therefore that the fraction of the ELM particles reaching the main chamber PFCs increases with the ELM size. Furthermore, the convective component of the electron heat flux is expected to have a similar behaviour as the electron temperature during ELMs does not vary significantly with the ELM size.

Our present database does not allow a quantitative study of the far SOL parameters dependence on the

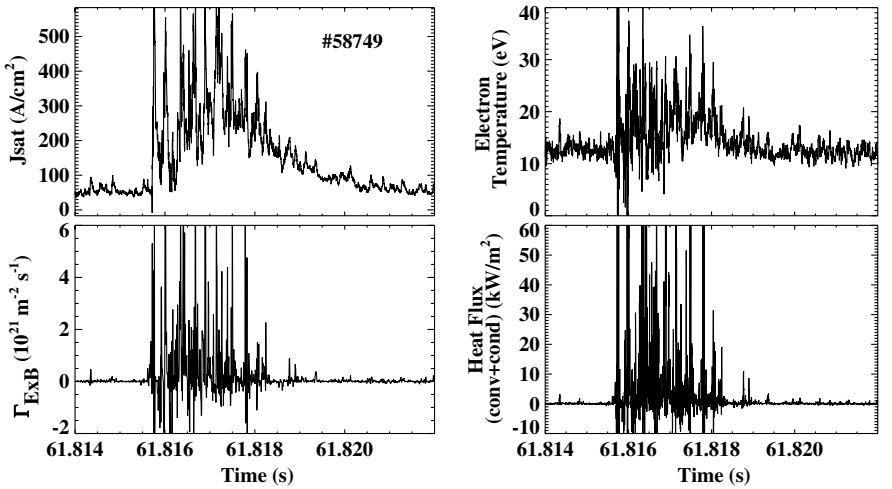

Fig. 6. Time evolution of J_{sat}, T_e and cross-field fluctuation induced particle and heat fluxes during a small type I ELM for a discharge with $I_p = 2$ MA, $B_T = 2.45$ T.

ELM losses. However, we know that: (i) the ELM radial velocity is high for the large amplitude ELMs, which are associated with more severe energy losses e.g. [13]; and (ii) the radial velocity is low for high frequency ELMs, characterized by small energy losses but significant particle losses e.g. [13]. Results suggest therefore that both the particle flux and radial velocity in the far SOL have a stronger dependence on the ELM energy loss than on the particle loss.

Probe data also show that the particle flux decreases rapidly outside the limiter radius (Fig. 2). The energy that reaches the main chamber wall during transient events, carried by both ions and electrons, will therefore be deposited in narrow radial region of the plasma facing components.

In summary, the particle and energy fluxes to the far SOL have been measured during ELMs and results show that both the far SOL J_{sat} and radial velocity increase with the ELM size. In spite of the large particle flux measured in the far SOL plasma during type I ELMs, the energy carried by electrons to the main chamber PFCs is very small ($\leqslant 5\%$ of the ELM losses). A detail study of the far SOL parameters dependence on the discharge characteristics is planed in plasmas optimised for measurements with the reciprocating probe.

Acknowledgments

This work, supported by the European Communities and 'Instituto Superior Técnico' under the Contract of Association between EURATOM and IST, has been carried out within the framework of the European Fusion Development Agreement. Financial support was also received from 'Fundação para a Ciência e Tecnologia' in the frame of the Contract of Associated Laboratory.

References

[1] T. Eich, R-3, these Proceedings. doi:10.1016/j.jnucmat.2004.09.051.
[2] A. Herrmann, 30th EPS conference on Controlled Fusion and Plasma Physics, St. Petersburg, 2003, ECA vol. 27A, p. 1.155.
[3] B. Gonçalves et al., Plasma Phys. Control. Fus. 45 (2003) 1627.
[4] W. Fundamenski, W. Sailer, Plasma Phys. Control. Fus. 46 (2004) 233.
[5] M.E. Fenstermacher et al., Plasma Phys. Control. Fus. 45 (2003) 1597.
[6] D.L. Rudakov, J.A. Boedo, et al., Plasma Phys. Control. Fus. 44 (2003) 717.
[7] J.A. Boedo et al., Phys. Plasmas, submitted for publication.
[8] A. Kirk, G.F. Counsell, et al., 30th EPS Conference on Controlled Fusion and Plasma Physics, St. Petersburg, July 2003, p. 3.21.
[9] C. Silva et al., Rev. Sci. Instrum. 75 (2004) 4314.
[10] A. Herrmann et al., J. Nucl. Mater. 313–316 (2003) 759.
[11] R.A. Richard et al., in preparation.
[12] D.W. Ross, Plasma Phys. Control. Fus. 34 (1992) 137.
[13] A. Loarte et al., Plasma Phys. Control. Fus. 45 (2003) 1549.